JOURNAL OF SOLID STATE CHEMISTRY 115, 395–406 (1995)

Out-of-Center Distortions around Octahedrally Coordinated d^0 Transition Metals

Martin Kunz[1] and I. David Brown

Institute for Materials Research, McMaster University, Hamilton, Ontario, Canada L8S 4M1

Received May 16, 1994; in revised form August 17, 1994; accepted August 19, 1994

The bond valence approach is used to model the characteristic out-of-center electronic distortions around d^0 transition metal cations in octahedral coordination. The distortions are influenced not only by the electronic structure of the cation but also by the structure of the bond network, by lattice incommensurations, and by cation–cation repulsion. These latter effects often determine whether a distortion will occur and, if so, in what direction. Once the direction of an expected out-of-center distortion is known, its magnitude can be modeled using modified bond valence network equations, where certain bonds are weighted to take into account the intrinsic inequality of the bonds in such a distorted coordination. The arguments are illustrated by examples. © 1995 Academic Press, Inc.

INTRODUCTION

Octahedrally coordinated d^0 transition metal cations such as Ti^{4+}, V^{5+}, and Mo^{6+} are usually found in distorted environments in which the cation is displaced from the center of the octahedron of ligands.

Similar distortions do not occur in the environments of main group elements of the same charge and size, as can be seen from a comparison between the structures of transition metal cations and their main group analogues. There are many examples, but two will suffice to make the point. The mineral titanite (sphene, $CaTiOSiO_4$) (1) has Ti^{4+} with distorted octahedral coordination (space group $P2_1/a$, Ti^{4+} site symmetry = 1) whereas its Sn analogue, the mineral malayaite ($CaSnOSiO_4$), which has the same structure, crystallizes in the higher symmetry space group $A2/a$ with Sn on a crystallographic inversion center that permits no out-of-center distortion.

A more dramatic example is $KTiOPO_4$ (2). Here, replacement of Ti^{4+} by Sn^{4+} (3) not only removes the distortion, but also decreases the second harmonic generation output to about 2% of that in $KTiOPO_4$. In this case, and in other similar cases, the out-of-center distortion around the d^0 transition metal is the driving force inducing optic and electric properties of technological importance (4).

The purpose of this paper is to explore the factors that influence the size and direction of these distortions. As a guideline to check the validity of our model we have set ourselves the task of finding a way to predict the observed bond lengths. The closer our prediction is to the observation, the more likely our analysis is to be correct.

A comparison of the out-of-center distortion found around various d^0 transition metals shows that the distortion increases with increasing formal charge and decreases with increasing size of the cation. This is illustrated in Fig. 1 which shows the frequency with which structures of a given distortion are found. Sc^{3+} (not shown) shows no distortion. Ti^{4+} and Ta^{5+} are found with a bimodal distribution, some structures having no distortion and others having distortions corresponding to an out-of-center shift of about 0.15 Å. Octahedrally coordinated V^{5+} is always strongly distorted and Cr^{6+} is never observed in octahedral coordination even though this would be expected on the basis of its size. However, its tetrahedral coordination can in many cases, e.g., in CrO_3, be interpreted as a heavily distorted octahedron, where the Cr^{6+} has moved so far toward an edge that the two long bonds can no longer be considered part of the coordination sphere. The same patterns can be seen in the heavier transition metals, but with a smaller tendency to distortion. Zr^{4+}, unlike Ti^{4+}, is always undistorted, and Mo^{6+}, unlike Cr^{6+}, is in many cases found in octahedral coordination.

The occurrence of out-of-center distortions by d^0 transition metal cations can be understood on the basis of the second-order Jahn–Teller theorem (6–10). The energy of the normally vacant cation d orbitals is lowered as the cation becomes smaller and more highly charged. If the energy is lowered sufficiently, the empty d orbitals are able to mix with the filled p orbitals of the ligands. In extended structures, this leads to a number of different electronic configurations with closely spaced energies

[1] To whom correspondence should be addressed at: Department of Earth and Space Sciences, University at Stony Brook, Stony Brook, NY 11794-2100.

0022-4596/95 $6.00

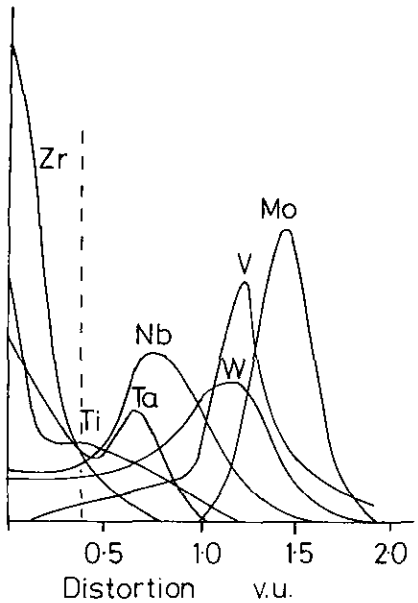

FIG. 1. The distribution of observed valence distortion in octahedral d^0 cations. The continuous lines are derived from histograms (0.1 vu bin size) obtained from the 50 most accurate coordination spheres found in the Inorganic Crystal Structure Database (5).

whose relative ordering depends on the chemical environment. Any near degeneracy in these configurations can usually be removed by a spontaneous distortion. However, it is not possible to make reliable quantitative predictions of the direction, magnitude, or even the occurrence of this distortion because it depends on the extended structure of the crystal. For this reason, we have used a simple empirical model to explore what determines the nature and origin of the distortions that occur in particular structures.

In analyzing the distortions around a number of d^0 transition metal cations, we have discovered that the second-order Jahn–Teller effect is not the only effect present. We have identified at least three other factors that work together symbiotically to stabilize the distortion: bond network effects, the stresses that result from the requirements of translational symmetry (lattice stresses), and cation–cation repulsion. In this paper we discuss each of these effects separately in Section 2 before showing how they combine in real crystals.

Structural details of a variety of compounds containing octahedrally coordinated d^0-transition metals were extracted from the Inorganic Crystal Structure Database (11). In Table 1 these are identified by their ICSD collection numbers. We used them to develop rules for determining whether a distortion will occur, and if so, in what direction the cation moves and how far. Finally in Section 3 we examine how well these rules are able to reproduce the observed out-of-center displacements.

2. SOURCES OF DISTORTION

In this section we discuss the four sources of distortion that are found in compounds containing octahedrally coordinated d^0 transition metal cations. In addition to the electronically driven distortion that is the focus of this paper, there are distortions that arise from the structure of the bonding network (the network of nearest neighbors) referred to as network distortions, there are distortions that arise from structural incommensurations which require two different parts of the structure to be strained in order to have the same lattice spacings, and there are distortions that arise from repulsion between second neighbors (cation–cation or anion–anion repulsion distortions).

2.1. Distortions Caused by the Bond Network

These can be predicted using the bond valence model (12) which treats a crystal as an infinite array of positively and negatively charged atoms (cations and anions) which are characterized by their atomic valence, i.e., their formal charge. Anions are connected to cations by bonds to form a network, with the bonds treated as vectors directed from the anion to the cation. Each bond is characterized by a bond valence which equals the amount of atomic valence contributed by each of its terminal atoms. In most compounds the bond valence (s) correlates with the bond length (r) through a relationship which can be expressed as

$$s = \exp(r_0 - r)/B), \qquad [1]$$

where r_0 and B are parameters whose values for many different bond types have been tabulated by Brown and Altermatt (13).

In most structures both the network, and the distribution of the atomic valence between the bonds, is determined by the principle of maximum symmetry, which states that, wherever possible, all the atoms and all the bonds will be chemically identical. This means, among other things, that the most stable bonding network will be one in which all the anions and all the cations are, as far as possible, crystallographically equivalent. It also means that the most stable coordination sphere is one in which all the bonds have, as far as possible, the same bond valence and hence the same bond length. The latter condition can be expressed quantitatively by the two network equations (12).

$$\text{Valence-sum rule: } \sum_j s_{ij} = V_i \qquad [2]$$

$$\text{Equal-valence rule: } \sum_{\text{loop}} s_{ij} = 0, \qquad [3]$$

TABLE 1

Comparison between Predicted and Observed Bond-Valences around Transition Metal Cations and Their Main-Group Analogues

A	B	C	D	E	F	G	H	I	J	K	L
					TiO_2 compounds						
Rutile	($P4_2/mnm$)	ICSD = 31321									
$O1^2$–$O1^4$	0.667	0.667	0	0	0	1	1	0.667	0.667	0.698	0.698
$O1^2$–$O1^4$	0.667	0.667	0	0	0	1	1	0.667	0.667	0.698	0.698
$O1^1$–$O1^3$	0.667	0.667	0	0	0	1	1	0.667	0.667	0.639	0.639
								Ti	0.030		
Anatase	($I4_1/amd$)	ICSD = 9852									
$O1^2$–$O1^2$	0.667	0.667	0	0	0	1	1	0.667	0.667	0.725	0.725
$O1^{10}$–$O1^{10}$	0.667	0.667	0	0	0	1	1	0.667	0.667	0.725	0.725
$O1^1$–$O1^9$	0.667	0.667	0	0	0	1	1	0.667	0.667	0.640	0.640
								Ti	0.050		
Brookite	($Pbca$)	ICSD = 36,408									
$O1^5$–$O2^8$	0.667	0.667	0	0	0	1	1	0.834	0.555	0.879	0.527
$O2^1$–$O1^1$	0.667	0.667	0	0.1	0.1	1.3	0.7	0.722	0.584	0.746	0.609
$O2^2$–$O1^8$	0.667	0.667	0	0.1	0.1	1.3	0.7	0.722	0.584	0.732	0.623
								Ti	0.031		
					AB_2O_6 structures						
Trirutile (B = Ta, A = Co)		($P4_2/mnm$)		ICSD = 203,095							
$O1^1$–$O1^2$	0.833	0.833	0	0	0	1	1	0.833	0.833	0.864	0.793
$O1^3$–$O1^4$	0.833	0.833	0	0	0	1	1	0.833	0.833	0.864	0.793
$O2^1$–$O2^3$	0.833	0.833	0	0	0	1	1	0.833	0.833	0.823	0.823
								Ta	0.029		
								Co	0.009		
Columbite (B = Nb, A = average of Mn, Fe, Co, Ni, and Zn)					($Pbcn$)		ICSD = 15,856; 15,858; 15,854; 15,852; 36,290				
$O2^1$–$O3^7$	1.167	0.667	0.500	0.100	0.600	1.4	0.6	1.236	0.545	1.329	0.378
$O1^1$–$O3^2$	0.917	0.667	0.250	0	0.250	1.4	0.6	1.030	0.545	1.025	0.627
$O3^1$–$O1^8$	0.667	0.917	−0.250	0.100	−0.150	1	1	0.908	0.735	0.882	0.610
							Nb	0.10			
Brannerite (B = V, A = average of Ca and Cd)				($C2/m$)	ICSD = 21,064; 9714						
$O2^1$–$O1^2$	1.167	0.917	0.250	0.100	0.350	1.6	0.1	1.518	0.093	1.536	0.100
$O1^1$–$O3^1$	0.917	0.667	0.250	0.100	0.250	1.6	0.7	1.387	0.519	1.368	0.542
$O3^2$–$O3^2$	0.667	0.667	0	0	0	1	1	0.741	0.741	0.792	0.792
							V	0.043			
					ABO_3 structures						
$MgTiO_3$ (Ilmenite structure)		($R\bar{3}$)		ICSD = 65,794							
$O1^4$–$O1^3$	0.667	0.667	0	0.081	0.081	1.3	0.7	0.867	0.467	0.870	0.477
$O1^5$–$O1^1$	0.667	0.667	0	0.081	0.081	1.3	0.7	0.867	0.467	0.870	0.477
$O1^6$–$O1^2$	0.667	0.667	0	0.081	0.081	1.3	0.7	0.867	0.467	0.870	0.477
							Ti	0.007			
							Mg	0.054			
$LiNbO_3$		($R3c$)		ICSD = 61,118							
$O1^4$–$O1^3$	0.667	0.667	0	0.081	0.081	1.4	0.6	1.167	0.500	1.098	0.554
$O1^5$–$O1^1$	0.667	0.667	0	0.081	0.081	1.4	0.6	1.167	0.500	1.098	0.554
$O1^6$–$O1^2$	0.667	0.667	0	0.081	0.081	1.4	0.6	1.167	0.500	1.098	0.554
							Nb	0.061			
							Li	0.047			
					Rotationally distorted perovskites						
$CaTiO_3$	($Pcmn$)	ICSD = 37,263 a_A/a_B = 0.946									
$O1^1$–$O1^2$	0.706	0.706	0	0	0	1	1	0.706	0.706	0.694	0.694
$O2^1$–$O2^5$	0.647	0.647	0	0	0	1	1	0.647	0.647	0.685	0.685
$O2^3$–$O2^7$	0.647	0.647	0	0	0	1	1	0.647	0.647	0.678	0.678
							Ti	0.029			
							Ca	0.073			
$NaTaO_3$	($Pcmn$)	ICSD = 23,329 a_A/a_B = 0.969									
$O2^3$–$O2^7$	0.833	0.833	0	0	0	1	1	0.833	0.833	0.870	0.870
$O1^2$–$O1^3$	0.833	0.833	0	0	0	1	1	0.833	0.833	0.852	0.852
$O2^1$–$O2^5$	0.833	0.833	0	0	0	1	1	0.833	0.833	0.842	0.842
							Ta	0.024			
							Na	0.049			

TABLE 1—*Continued*

A	B	C	D	E	F	G	H	I	J	K	L
$NaNbO_3$	(*Pbcm*)	ICSD = 23,239 a_A/a_B = 0.973									
$O3^7$–$O4^7$	0.830	0.833	−0.003	0	−0.003	1.4	0.6	1.078	0.549	1.163	0.584
$O4^1$–$O3^1$	0.833	0.830	0.003	0	0.003	1	1	0.916	0.770	0.902	0.688
$O2^1$–$O1^1$	0.856	0.817	0.039	0	0.039	1	1	0.850	0.837	0.859	0.830
							Nb	0.051			
							Na	0.065			
					Undistorted perovskite						
$SrTiO_3$	($Pm\bar{3}m$)	(16) a_A/a_B = 1.001									
$O1^1$–$O1^1$	0.667	0.667	0	0	0	1	1	0.667	0.667	0.691	0.691
$O1^5$–$O1^5$	0.667	0.667	0	0	0	1	1	0.667	0.667	0.691	0.691
$O1^9$–$O1^9$	0.667	0.667	0	0	0	1	1	0.667	0.667	0.691	0.691
							Ti	0.024			
							Sr	0.009			
					Out-of-center distorted perovskite						
$BaTiO_3$	(*P4mm*)	ICSD = 23,758 a_A/a_B = 1.061									
$O1^1$–$O1^1$	0.667	0.667	0	0	0	1.3	0.7	0.867	0.467	0.872	0.385
$O2^1$–$O2^1$	0.667	0.667	0	0	0	1	1	0.667	0.667	0.606	0.606
$O2^5$–$O2^5$	0.667	0.667	0	0	0	1	1	0.667	0.667	0.606	0.606
							Ti	0.060			
							Ba	0.065			
$KTaO_3$	($Fm\bar{3}m$)	(15) a_A/a_B = 1.086									
$O1^1$–$O1^1$	0.833	0.833	0	0	0	1	1	0.833	0.833	0.818	0.818
$O1^5$–$O1^5$	0.833	0.833	0	0	0	1	1	0.833	0.833	0.818	0.818
$O1^9$–$O1^9$	0.833	0.833	0	0	0	1	1	0.833	0.833	0.818	0.818
							Ta	0.015			
							K	0.073			
$KNbO_3$	(*Amm2*)	ICSD = 9533		a_A/a_B = 1.093							
$O2^1$–$O2^1$	0.833	0.833	0	0	0	1.4	0.6	1.167	0.500	1.107	0.498
$O2^2$–$O2^2$	0.833	0.833	0	0	0	1.4	0.6	1.167	0.500	1.107	0.498
$O1^1$–$O1^1$	0.833	0.833	0	0	0	1	1	0.833	0.833	0.794	0.794
							Nb	0.041			
							K	0.072			
Titanyl and vanadyl compounds (in the following compounds the axial bonds that form the chain are listed first)											
$V2O_5$	(*Pnma*)	ICSD = 60,767									
$O1^1$–$O1^1$	1.000	1.000	0	0	0	1.6	0.1	1.882	0.118	1.847	0.069
$O3^1$–$O2^1$	1.000	0.667	0.333	0	0.333	1.6	0.7	0.998	0.518	1.068	0.560
$O2^4$–$O2^4$	0.667	0.667	0	0	0	1	1	0.741	0.741	0.818	0.818
							V	0.061			
β-$SbOPO_4$	(*C2/c*)	ICSD = 201,743									
$O1^1$–$O1^3$	1.000	1.000	0	0	0	1	1	1.000	1.000	1.112	1.112
$O2^2$–$O2^4$	0.750	0.750	0	0	0	1	1	0.750	0.750	0.889	0.889
$O3^4$–$O3^2$	0.750	0.750	0	0	0	1	1	0.750	0.750	0.874	0.874
							Sb	0.126			
							P	0.037			
α-$NbOPO_4$	(*P4/n*)	ICSD = 24,110									
$O1^1$–$O1^1$	1.000	1.000	0	0	0	1.4	0.6	1.400	0.600	1.415	0.330
$O2^7$–$O2^8$	0.750	0.750	0	0	0	1	1	0.750	0.750	0.854	0.854
$O2^6$–$O2^5$	0.750	0.750	0	0	0	1	1	0.750	0.750	0.854	0.854
							Nb	0.140			
							P	0.022			
α-$VOPO_4$	(*P4/n*)	ICSD = 629									
$O1^1$–$O1^1$	1.000	1.000	0	0	0	1.6	0.1	1.882	0.118	1.836	0.055
$O2^1$–$O2^2$	0.750	0.750	0	0	0	1	1	0.750	0.750	0.776	0.776
$O2^3$–$O2^4$	0.750	0.750	0	0	0	1	1	0.750	0.750	0.776	0.776
							V	0.038			
							P	0.072			

TABLE 1—*Continued*

A	B	C	D	E	F	G	H	I	J	K	L
β-$VOPO_4$	(*Pnma*)	ICSD = 9413									
$O4^1$–$O4^3$	1.000	1.000	0	0	0	1.6	0.1	1.883	0.118	1.902	0.119
$O2^3$–$O3^1$	0.750	0.750	0	0	0	1.6	0.7	0.910	0.611	0.872	0.766
$O1^1$–$O1^8$	0.750	0.750	0	0	0	1	1	0.740	0.740	0.798	0.798
							V	0.074			
							P	0.084			
$CaTiOSiO_4$	($P2_1/a$)	ICSD = 12,131									
$O1^1$–$O1^4$	0.779	0.779	0	0	0	1.3	0.7	1.013	0.545	1.140	0.650
$O4^2$–$O2^4$	0.649	0.649	0	0	0	1	1	0.649	0.649	0.632	0.622
$O3^1$–$O5^3$	0.572	0.572	0	0	0	1	1	0.572	0.572	0.584	0.567
							Ti	0.069			
							Si	0.037			
							Ca	0.053			
$KTiOPO_4$	($Pn2_1/a$)	ICSD = 20,970									
$O5^3$–$O1^1$	0.758	0.598	0.160	0	0.160	1.3	0.7	0.990	0.456	1.292	0.405
$O2^4$–$O6^3$	0.599	0.757	−0.159	0	−0.159	1.3	0.7	0.729	0.532	0.674	0.645
$O8^3$–$O7^3$	0.686	0.603	0.083	0	0.083	1	1	0.688	0.606	0.627	0.534
$O6^3$–$O5^1$	0.768	0.768	0	0	0	1.3	0.7	0.997	0.538	1.208	0.472
$O9^3$–$O10^1$	0.611	0.611	0	0	0	1	1	0.612	0.612	0.668	0.618
$O4^2$–$O3^1$	0.635	0.607	0.028	0	0.027	1	1	0.635	0.607	0.642	0.538
							Ti	0.118			
							P	0.028			
							K	0.084			

Note. (A) Terminal atoms: the first number is the atom identifier, the superscript is the symmetry operator. The two terminal atoms on the same line are on opposite corners of the octahedron; (B and C) Predicted bond valences using the unweighted network equations ([2] and [3]); (D) Distortion vector **D** predicted from bond valences (Column B and C); (E) Distortion vector **E** predicted from the cation–cation repulsions; (F) Resultant distortion vector; (G) and H) Weights assigned to the bonds; (I) and J) Predicted bond valences using weighted network equations (Eqs. [4] and [5]); K) and L) Observed bond valences. The standard deviation between the observed and predicted bond valences is given in col. J on the last lines of each entry.

where V_i is the atomic valence of atom i and, s_{ij} is the bond valence between atoms i and j. The valence sum rule (Eq. [2]) requires that at each atom the sum of the bond valences equal the atomic valence. It is less clear that Eq. [3] leads to the condition that the valences of the bonds incident at a given atom should be as equal as possible, but this can be demonstrated (14). Once the topology of the bond network is known, the network equations lead to a unique distribution of the atomic valences between the bonds. Equation [1] can then be used to predict the lengths of the bonds (ideal bond lengths).

Although observed structures tend to form bond networks in which all the ions (particularly the anions) are equivalent and all the bonds have the same valence, it is certainly possible to construct networks in which this is not the case. Figure 2 shows two networks both corresponding to a compound with the formula $A^{2+}B_2^{5+}O_6$. In both networks all the cations are 6-coordinate and the anions 3-coordinate. In network (a), all the O^{2-} ions are equivalent, all the bonds formed by A^{2+} are the same, and all the bonds formed by B^{5+} are the same. This is the network that would be expected from the principle of

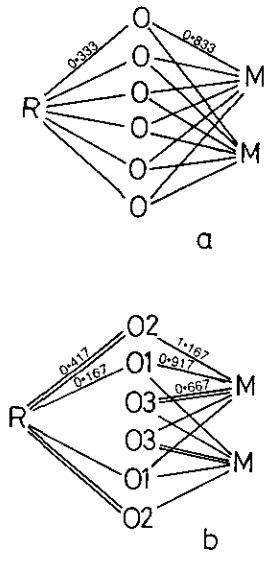

FIG. 2. Finite bond network graphs for $A^{2+}B_2^{5+}O_6$ structures: (a) graph of trirutile; (b) graph of columbite and brannerite. The numbers are bond valences predicted using Eqs. [2] and [3].

maximum symmetry and it is the network adopted, for example, by $ZnSb_2O_6$ which has the trirutile structure. Network (b) differs from (a) in that two A–O bonds have been interchanged with two B–O bonds. The coordination numbers are still the same, but the anions are no longer equivalent and the bonds around each cation are no longer the same. This network is adopted by ZnV_2O_6 (brannerite structure) and shows that the tendency of V^{5+} to favor a distorted environment is sufficiently strong so that it results in the adoption of a bond network that is itself intrinsically distorted. As we shall see below, the intrinsic distortion of the network and the second-order Jahn–Teller distortion of V^{5+} are mutually supportive.

Ideal bond lengths determined in this way are close to those found in most compounds whose coordination spheres show no large distortion, and they provide a useful reference from which to measure the distortions found in the d^0 transition metal compounds (see columns B and C in Table 1). Since the bond–valences are measures of the strength of bonding, it is convenient to make the comparison between the ideal and the observed structures in terms of their bond valences rather than their bond lengths. For this purpose, in the structures examined in this study, observed bond valences were calculated from the observed bond lengths using Eq. [1] with the parameters of (13), and these were compared with the ideal bond valences calculated using Eqs. [2] and [3]. The size of an out-of-center distortion (whether predicted or observed) can be expressed by a vector **D**, whose components correspond to the differences between the valences of pairs of *trans* bonds, viz.: $\mathbf{D} = \{s(x) - s(-x), s(y) - s(-y), s(z) - s(-z)\}$. The distortion vector thus gives both the magnitude and the direction of the distortion relative to x, y, and z axes chosen parallel to the bonds in the octahedron. The distortion calculated from the bond valences predicted using the network equations (Eqs. [2] and [3]) is called the "network distortion." It reflects the asymmetry in the bond network itself and therefore includes contributions to the distortion from second and third bonded neighbors.

2.2. *Distortions Caused by Structural Incommensurations (Lattice Stresses)*

A second cause of distortion of cation environments arises in compounds where it is impossible to find locations for the atoms in three-dimensional space that give bond lengths equal to the ideal bond lengths predicted using the network equations. An example of this situation is found in the perovskite, $BaTiO_3$. The cubic symmetry of the perovskite structure requires that the ratio of the lengths of the Ba–O and Ti–O bonds be exactly $\sqrt{2} = 1.41$, but the ratio of the ideal bond lengths calculated from Eqs. [1], [2], and [3] is $2.95/1.96 = 1.50$. The Ba–O bonds are too long and the Ti–O bonds too short for an ideal fit. Consequently, in order to exist in the cubic phase, the Ba–O bonds must be compressed and the Ti–O bonds stretched, resulting in the sum of the bond valences (calculated using Eq. [1]) around Ti^{4+} being only 3.64 instead of 4.00. In this phase, therefore, even though the equal valence rule (Eq. [3]) is observed, the valence sum rule (Eq. [2]) is not. In practice, the valence sum rule is a more stringent requirement than the equal valence rule so that, at lower temperatures, the Ti atom moves out of center in its coordination sphere. This has the effect of satisfying the valence sum rule at the expense of the equal valence rule. The reason why this distortion raises the valence sum lies in the form of Eq. [1]: it leads to the distortion theorem (12) which states that, if some of the Ti–O bonds are lengthened and others shortened in such a way that the average bond length remains the same, the average bond valence increases. This effect is quite general: the environment of any cation whose bonds are stretched as a result of structural incommensuration will tend to distort in order to satisfy the valence sum rule. In the case of $BaTiO_3$, the lattice stress distortion is supported by the second-order Jahn–Teller distortion. By contrast, $BaSnO_3$ remains cubic, in part because Sn is slightly larger than Ti so the lattice stress is less, and in part because Sn is unable to benefit from a second-order Jahn–Teller distortion.

The lattice stress does not show any preference for the direction in which the distortion will occur. Usually the direction will be determined by other mechanisms such as the network distortion. In $BaTiO_3$, the distortion breaks the cubic symmetry and the distortion may occur in any of the equivalent cubic directions. Unless limited by other factors, the size of the distortion will be determined by the need to ensure that the valence sum rule is satisfied around the cation.

2.3. *Distortion Caused by Cation–Cation Repulsion*

When two coordination octahedra share edges or faces, the cations are brought into contact and tend to relax by moving away from each other. The magnitude of the repulsion between the cations is difficult to estimate, the more so because, in the compounds examined in this study, cation–cation repulsion was only one of the effects leading to distortion. In practice, the size of the cation–cation repulsion is not important since the cations are usually sufficiently well separated by other distortion effects, but the direction is important in determining the direction of the second-order Jahn–Teller distortion. This is illustrated by the three polymorphs of titania (TiO_2), rutile, anatase, and brookite. All three share the same bond network, which is symmetric about Ti^{4+}, so none of the structures show network distortions. Lattice

stress distortions are also absent. In rutile the octahedra share opposite edges and in anatase they share four edges arranged with $\bar{4}$ symmetry. In both these structures cation–cation repulsion cancels leaving Ti^{4+} in the center of its octahedron. However, brookite has an asymmetric arrangement of shared edges, the cation–cation repulsions do not cancel and Ti^{4+} is displaced from the center of its octahedron. As discussed in Section 3.1, the direction of the observed displacement is determined by the cation–cation repulsion but the magnitude is determined by the second-order Jahn–Teller effect.

We represent the cation–cation repulsion by a distortion vector, **E**, having a magnitude of 0.14 vu (a value chosen to give the best bond valence predictions in the procedure described in Section 3), directed antiparallel to the line joining two cations whose octahedra share edges or faces. Where an octahedron shares several edges, the individual distortion vectors are added.

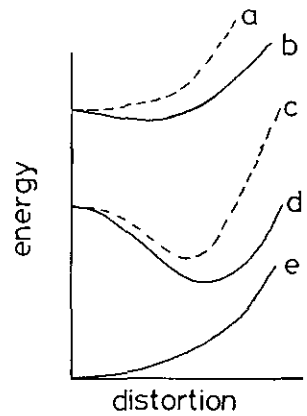

FIG. 3. Energy versus distortion coordinate for a compound with a symmetric structural energy: (a) total energy for a large *d–p* gap; (b) electronic energy for a large *d–p* gap; (c) total energy for a small *d–p* gap; (d) electronic energy for a small *d–p* gap; (e) symmetric structural energy.

2.4. Distortions Caused by Electronic Effects

The lowering of the energy of the vacant *d* orbitals of a d^0 transition-metal cation with increasing ionic charge allows the orbitals to mix with the filled ligand *p* orbitals. Depending on the involvement of these *p* electrons in bonding to other atoms, one may have an instability caused by a near-degeneracy of molecular orbitals close to the Fermi level, a degeneracy which can be removed by a spontaneous distortion (6, 7). There are two necessary conditions for the occurrence of a second-order Jahn–Teller distortion: First the energy gap between highest occupied (HOMO) and lowest unoccupied molecular orbitals (LUMO) needs to be small. Secondly, there has to be a distortion mode of the same symmetry as the HOMO to LUMO transition. While the latter condition is always satisfied in octahedrally coordinated d^0 transition metals, the fulfillment of the first condition is dependent on both the charge and size of the cation and on the way the ligands are bonded to the rest of the structure.

In addition to the energy contributed by the electronic distortion, the total energy of the crystal also contains contributions from structural effects which, by the principle of maximum symmetry, are expected to work against distortion unless any of the mechanisms discussed above are present. Any lowering of the electronic energy caused by distortion has to compete with a possible increase in the structural energy. Figures 3 and 4 show these energies schematically for various situations as a function of the distortion coordinate. In order that an out-of-center distortion can occur, either the electronic energy must be lowered by more than the structural energy is raised (Fig. 3), or the structural energy must itself have a minimum that corresponds to a distorted structure (Fig. 4). In cases where both types of distortion are present, the two effects usually support each other: one rarely finds cases where the two effects are opposed since structures in which the various effects support each other are intrinsically more stable than those where they are in competition.

The magnitude of the electronic effect depends inversely on the size of the energy gap between HOMO and LUMO. It will be reduced as the LUMO, which has mostly cation *d* character, is lowered in cations with higher charge and smaller size. Thus Sc^{3+} and Zr^{4+}, where the structural energy dominates, show no tendency to distort, but V^{5+}, and Mo^{6+}, where the electronic energy dominates, are always distorted. In between lie Ti^{4+}, Ta^{5+}, and Nb^{5+} which are sometimes found in distorted, and sometimes in undistorted environments, depending on the nature of the structural energy.

Because one needs to take into account the extended crystal structure in calculating the electronic distortion, it

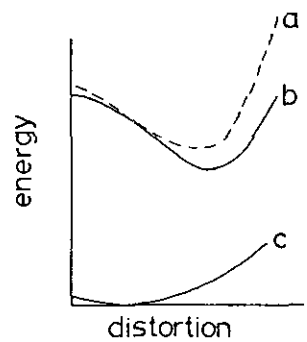

FIG. 4. Energy versus distortion coordinate for a compound with an asymmetric structural energy: (a) total energy; (b) electronic energy; and (c) structural energy.

is impractical to use quantum mechanics to predict its extent. Consequently, we have adapted the bond valence model by introducing a weighted form of the network equations ([2] and [3])

$$\sum_j s_{ij} = V_i \quad [4]$$

$$\sum_{\text{loop}} s_{ij}/C_{ij} = 0, \quad [5]$$

where C_{ij} is an arbitrarily chosen weighting constant for the bond ij, being larger for bonds that are expected to be strong and smaller for bonds that are expected to be weak. If C_{ij} is set to 1.0 for all bonds, Eqs. [4] and [5] reduce to Eqs. [2] and [3]. The values of C_{ij} used in this study are given in Table 2 and the way in which they are assigned is discussed in the next section. These weights are empirical parameters that appear to be transferable between most compounds of a given cation, but we do not attempt to interpret them in electronic terms.

2.5. *Combining These Effects*

Of the four distorting effects described above, only the bond network and cation–cation repulsions are able to direct the distortion. The other two effects, the lattice stress and electronic distortion, show no directional preference. It is, therefore, the former, if present, that will determine the direction in which the cation will move out of center.

All four effects will influence the magnitude of the distortion, but the total distortion is not just the sum of the individual contributions, since the distortion produced, for example, by the electronic effect may be sufficient to relax both the lattice stress and the cation–cation repulsions as well. For this reason, it is often possible to model the magnitude of the distortion using only Eqs. [4] and [5] with the values of C_{ij} given in Table 2.

The procedure used for modeling is then as follows: The direction of the distortion must first be determined by adding the distortion vector **D** predicted from the (unweighted) network equations (Table 1, column D) and the distortion vector **E** predicted from the cation–cation repulsion (Table 1, column E), to give the resultant shown in column F of Table 1. Any bonds that lie within 65° of the resultant distortion vector are given the higher weight (C_{ij}) shown in Table 2 and the bonds *trans* to these are given the corresponding lower weight. Bonds lying more than 65° from the distortion vector are given unit weight. Equations [4] and [5] are then used to predict the bond valences (Table 1, columns I and J).

The results of this procedure can be summarized in the following statements:

(i) If the electronic distortion is weak (Sc^{3+}, Zr^{4+}) there are also no structural distortions observed.

(ii) If the electronic distortion is of moderate strength (Ti^{4+}, Nb^{5+}, Ta^{5+}), distortions will only occur if structural distortions are present. The direction of the distortion is determined by the asymmetry in the bond network and cation–cation repulsion if these are present. If only lattice stress is present, the distortion can occur in either of two or more symmetry breaking directions.

(iii) If the electronic distortion is large (V^{5+}, Mo^{6+}, W^{6+}) a distortion is observed in any case. Usually compounds of these cations will crystallize with a bond network that supports and directs the distortion. Compounds in which no structural distortion is present are rare.

(iv) A consequence of (i) to (iii) above is that the absence of any source of structural distortion will result in the d^0 cation being in an undistorted environment, and this can be used as a criterion to determine when an electronically distorted structure can be expected.

TABLE 2
Values of C_{ij} for Some d^0 Transition Metals.

Ion	C_{ij} (strengthened bond)	C_{ij} (weakened bond)
Ti^{4+}	1.3	0.7
Ta^{5+}	1.3	0.7
Nb^{5+}	1.4	0.6
V^{5+}[a]	1.6	0.1
	1.6	0.7

Note. In each case, the weakened bond is *trans* to the strengthened bond.

[a] The extreme distortion observed around V^{5+} required two different C_{ij} pairs for the strongest and second strongest bonds.

3. EXAMPLES OF THE APPLICATION OF THE MODEL

In this section we apply these principles to a number of systems of related structures to see how well the predictions of bond length work. Each of the subsections below discusses a group of related structures and the results of the calculations are shown in Table 1 which, for each pair of *trans* bonds, gives the unweighted network predictions (columns B and C), the network distortion (D), the cation–cation repulsion distortion (E), the resultant predicted distortion vector (F), the weights assigned (G and H), the predictions of the weighted network equations (I and J), and the observed valences (K and L). The root mean square deviations between the predicted and observed bond valences around each cation are also shown in column (I).

3.1. *Polymorphs of TiO_2*

As mentioned above, TiO_2 occurs in three polymorphs, all of which have a symmetric bond graph and none of

which shows lattice strain. The octahedra in rutile and anatase share edges arranged in a symmetric way, the cations lying on positions of $\bar{1}$ and $\bar{4}$ symmetry respectively, so that the cation–cation repulsions cancel. The octahedra in both these compounds are undistorted. The third polymorph, brookite, differs only in that the octahedral edges are shared asymmetrically, forcing the Ti^{4+} ion away from the center of the octahedron. In this case the Ti^{4+} environment is distorted. The predictions are shown in Table 1. The assignment of weights is unambiguously given by the cation–cation repulsion, but interestingly the bond that is both predicted and observed to be the strongest is not one of those given high weight, a fact that lends credibility to the model.

3.2. *Compounds with the Formula* $A^{2+}B_2^{5+}O_6$

Many of the compounds with this formula crystallize with the trirutile structure, a structure derived from rutile with three Ti^{4+} cations replaced by A^{2+} and $2B^{5+}$ cations. The 5-valent B cations found with this formula include V^{5+}, Nb^{5+}, Ta^{5+}, As^{5+}, and Sb^{5+} but not all of these form trirutiles; three additional structure types are also observed, a hexagonal structure and the columbite and the brannerite structures. Which of these is adopted has much to do with the tendency for the cation to undergo electronically driven distortions. The trirutile and hexagonal structures have the symmetrical bond graph shown in Fig. 2a while columbite and brannerite have the less symmetric bond graph shown in Fig. 2b for which network distortions are predicted. All the structures are composed of chains of edge-sharing octahedra. In the hexagonal structure the chains are further edge-linked to form hexagonal sheets in a way that results in most of the cation–cation repulsions canceling. Trirutile, columbite, and brannerite each contain differently linked chains of BO_6 octahedra (Fig. 5). In trirutile (Fig. 5a), as in rutile, the chains share opposite edges in a way that results in the cation–cation repulsions canceling. In columbite the octahedra share semiadjacent edges (Fig. 5b), and in brannerite they share adjacent edges (Fig. 5c) and are further linked by shared edges into sheets. In columbite, and particularly in brannerite, out-of-center distortions are predicted as a result of cation–cation repulsion. The agreement between prediction and observation for typical structures of each kind is generally good. However, because the structures consist of parallel chains of A and B cations that in general are not commensurate, the real structures show complex (but predictable) lattice strains whose effects are not included in Table 1.

Because neither the bond network nor the cation–cation repulsion lead to out-of-center distortions in the trirutile and hexagonal structures, these structures are adopted by compounds in which B = As, Sb, and Ta. Columbite is adopted by compounds in which B = Nb and brannerite, which, because of lattice stress, shows the largest tendency to distortion, is adopted by compounds with B = V.

3.3. *Compounds of* ABO_3

These compounds fall into three structure classes: the ilmenite structure in which both A and B are 6-coordi-

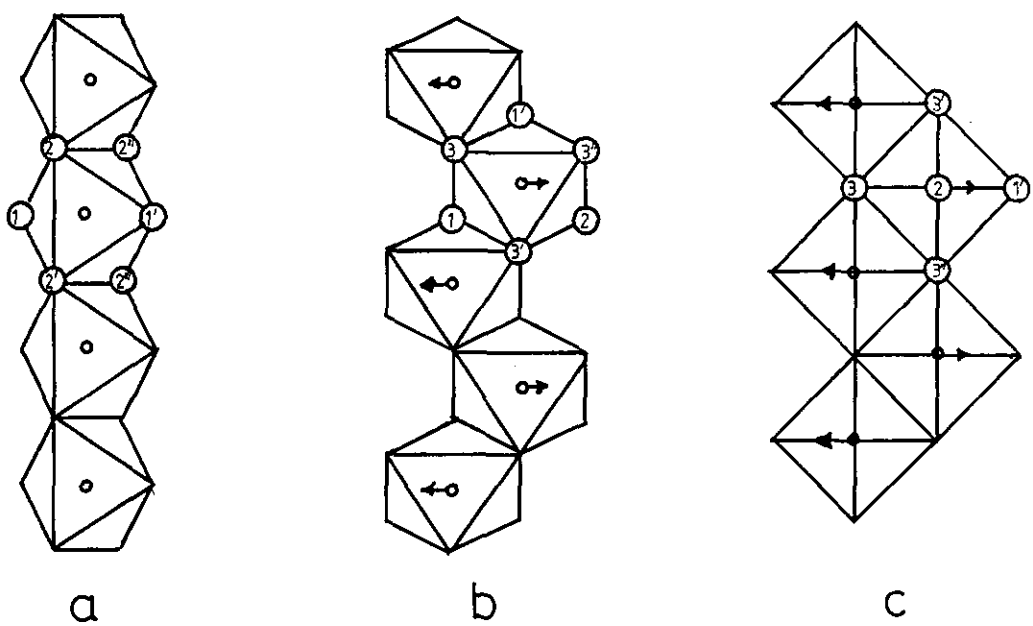

FIG. 5. Chains of edge sharing octahedra: (a) straight chains in trirutile; (b) partially staggered chains in columbite; and (c) fully staggered chains in brannerite (atom O1 lies behind atom O2). The arrows indicate the direction of cation displacements arising from cation–cation repulsion.

nate, the $LiNbO_3$ structure, which differs from the ilmenite structure only by a different (acentric) cation-ordering scheme, and the perovskite structures in which A is 8- to 12-coordinate.

In the ilmenite structure, adopted by, e.g., $MgTiO_3$ and the $LiNbO_3$-structure, AO_6 and BO_6 octahedra share faces. The unweighted network equations predict no distortion but the cation–cation repulsion across the shared face results in both A and B atoms moving away from each other along the threefold axis. This is modeled, as shown in Table 1, by giving low weight to the three B–O bonds directed to the shared face. The agreement is satisfactory even though the weighted network model does not predict the observed out-of-center displacement of the A atoms.

The perovskite structure is a simple cubic network of corner linked BO_6 octahedra with the A atom in the center of the cube formed by the B atoms. The A atoms are 12-coordinate and the B atoms 6-coordinate. There are no shared edges or faces between the octahedra so cation–cation repulsion is absent, but the ideal cubic perovskite structure is, in almost every case, a strained structure, because the A–O and B–O bond lengths are both determined by the single free parameter in the structure, the lattice spacing, a_0. Lattice stress must therefore be present if the ratio $r(A\text{–O})/r(B\text{–O})$ is not exactly $\sqrt{2}$. The degree of mismatch can best be expressed by the ratio of the lattice dimension predicted from the ideal A–O bond length ($a_A = \sqrt{2} \times r(A\text{–O})$) and the lattice dimension predicted from the ideal B–O bond length ($a_B = 2 \times r(B\text{–O})$). If a_A/a_B is less than 1.0 the A atoms are too small, the A–O bonds will be in tension and the B–O bonds in compression. If a_A/a_B is greater than 1.0 the B–O bonds will be in tension and the A–O bonds in compression. According to the distortion theorem, the structure will relax to give a distorted environment around the atom whose bonds are in tension. This gives rise to two kinds of distorted structures. For compounds with $a_A/a_B < 1.0$, the linked BO_6 octahedra twist so as to increase the length of some A–O bonds while decreasing the length of the others. For compounds with $a_A/a_B > 1.0$ the B atom goes out-of-center in its octahedron, a distortion that is consistent with the electronic distortions expected around B transition metal ions. It is convenient to deal with these two cases separately and then, finally, to consider the special case of $SrTiO_3$ where $a_A/a_B = 1.0$.

Rotationally distorted perovskites. Rotation of the network of BO_6 octahedra is expected for perovskites in which $a_A/a_B < 1.0$, that is for compounds with relatively small A atoms such as Ca and Na. The rotation can occur in varying degrees around two orthogonal axes, so that the nature and extent of the rotation will be different in each compound and, indeed, will vary with temperature. For convenience we consider only the room temperature structures. Although the A atom still has 12 neighboring O atoms, some of them are at distances that are normally not regarded as bonding, though the boundary between bonding and nonbonding distances is somewhat arbitrary. Different choices for the boundary will result in different bond networks and different predictions of bond valence. This is not a serious problem, since the differences are only of order 0.04 vu, but it introduces some uncertainty into the predictions made with the network equations since these depend critically on which atoms are connected by bonds. In this study a distance is considered a bond if its observed bond valence exceeds $0.038 \cdot V$, where V is the oxidation state of the cation.

Predictions are given for three rotationally distorted perovskites, one each with $B = Ti^{4+}$, Ta^{5+}, and Nb^{5+}. The compressive lattice strain in the B–O bonds will inhibit any tendency for the B atom to go out of center. It is not surprising, therefore, to find that both $CaTiO_3$ and $NaTaO_3$ adopt structures in which the B atom is restricted by symmetry to be at the center of its octahedron. The situation in $NaNbO_3$ is more complex. In this compound, not only is Nb intrinsically more unstable to electronic distortion than either Ti or Ta, but the ratio a_A/a_B is also closer to 1.0, indicating that the lattice-induced compression in the Nb–O bonds is smaller. At least five noncubic phases have been reported for $NaNbO_3$, and the phase observed at room temperature has Nb displaced out of center in its octahedron, in addition to the expected rotation. The unweighted network equations predict a small out-of-center displacement for Nb but, as mentioned above, this displacement is largely an artifact of the arbitrary cutoff in the coordination sphere of Na. The observed distortion adopts a different direction and, in the absence of any other criterion, the weights have been assigned to match this observation. In all three of these structures the agreement between the predicted and observed valences is good (Table 1).

Out-of-center distorted perovskites. Perovskites with $a_A/a_B > 1.0$ are expected to distort with B moving out of center in its coordination sphere. Such a distortion has the potential of being ferroelectric, as observed in $BaTiO_3$ and $KNbO_3$, both of which have three ferroelectric noncubic phases with Ti displaced toward a corner, an edge, and a face of the octahedron, respectively, as the temperature is reduced. Our model does not predict which of these phases will be the most stable, but is does allow us to make predictions of the bond lengths in each case. In this analysis we examine the room temperature structures. For $BaTiO_3$ this is the tetragonal phase in which Ti^{4+} moves toward the corner of the octahedron and for $KNbO_3$ it is the orthorhombic phase in which Nb^{5+} moves toward the edge of the octahedron. Because neither bond network nor cation–cation repulsion distortions are present, there is no preferred direction for the

distortion and it is a matter of chance which way it will occur. The choice of which bonds to weight is therefore arbitrary. Satisfactory agreement between the predicted and observed bond valence is found for both compounds when weights are assigned to those bonds which are observed to be the strongest and the weakest. However, the out-of-center distortion does not completely remove the lattice strain. Even with the bond distortion, the A–O bonds are still strongly compressed (bond valence sum at Ba^{2+} = 2.73 vu, at K^+ = 1.80 vu) and the B–O bonds are stretched (bond valence sums at Ti^{4+} = 3.68 vu, at Nb^{5+} = 4.80 vu).

Surprisingly, $KTaO_3$ remains cubic at least down to 1 K in spite of the large a_A/a_B ratio but the bond strain in cubic $KTaO_3$ is not much different from that in orthorhombic $KNbO_3$ with the valence sum at K = 1.87 vu and at Ta = 4.91 vu. In this compound the cubic structure must be stabilized by the high compressibility of the K atoms but recent work (15) suggests that, despite the macroscopic cubic symmetry, the local symmetry around Ta is distorted in the same way as it is in $SrTiO_3$, as discussed below.

$SrTiO_3$. Strontium titanate is unusual in that the ratio a_A/a_B is almost exactly 1.00 so there is no lattice strain to produce a distortion. At room temperature it is cubic but it undergoes a rotational distortion below 104 K. The predicted bond valences for the undistorted structure shown in Table 1 agree well with those observed. However, recent experimental results (16) suggest that at room temperature both the Ti and O atoms are displaced away from their ideal cubic positions in a way that is consistent with a model in which the Ti atom is randomly displaced by 0.12 Å from the center of a regular octahedron of O atoms, exactly the displacement predicted using weighted bond network equations.

3.4. Titanyl and Vanadyl Structures

The characteristic features of these compounds, are single chains of corner-sharing BO_6 octahedra linked by tetrahedral AO_4 ions. Since the octahedra only share corners, there is no cation–cation repulsion.

Because, in most of these compounds, adjacent B atoms along the chains are related by symmetry, the network equations usually predict that all the B–O bonds along the chain have the same valence. Under these circumstances, one might expect undistorted coordination, at least for $B = Ti^{4+}$, Ta^{5+}, and possibly Nb^{5+}. However, displacing the B atoms along the chain (axial direction) does not affect any other bonds in the structure and, hence, the distortion causes no loss of structural energy. In modeling these compounds we assume that the axial direction is the direction of major distortion. Distortions in the other (equatorial) directions are not expected unless specifically required by the structure.

In V_2O_5 the major distortion is along the chain, but the unweighted network equations indicate that a distortion is also expected along one of the equatorial axes. The network equations with both these sets of bonds weighted gives satisfactory agreement with observation (Table 1).

Compounds with the formula $BOAO_4$ crystallize in two different forms. Compounds with the α structure have straight BO chains (O–B–O = 180°) with each of the AO_4 ions linking four different chains. In the β structure the AO_4 ion links only three chains, but to one of these it forms bonds to two adjacent B atoms, resulting in the chain being bent with a B–O–B angle of around 135°. Many compounds are known with one or the other of these structures. $NbOPO_4$ adopts the α structure and $TaOPO_4$ the β, while $VOPO_4$ occurs in both forms. The structure of $TaOPO_4$ is omitted from Table 1 since its structure is not sufficiently well determined, but $SbOPO_4$ is included as an example of a compound where distortion is neither expected nor found.

The tetragonal α structure has a large lattice stress, since the c axis length is determined by both the length of the axial B–O bonds and by the spacing between the AO_4 ions which form columns with interionic O–O contacts of only 2.8–2.9 Å. The AO_4 columns are compressed and the BO chains stretched, resulting in the distortion being enhanced by the lattice stress. For this reason, the environment of V in α-$VOPO_4$ is more distorted than in β-$VOPO_4$, and the distortion in α-$NbOPO_4$ is larger than predicted (Table 1).

Related to the $BOAO_4$ structures are the $CBOAO_4$ structures in which additional C ions have been introduced into the spaces between the chains and the anions. $CaTiOSiO_4$, titanite, has a structure closely related to β-$BOAO_4$ but $KTiOPO_4$ and $KTiOAsO_4$ have a different structure with the AO_4 tetrahedra linking only two chains and the chains running along two mutually perpendicular directions. The chains in the latter case also differ from those in the other structures in that alternate BO_6 octahedra link through *cis* bonds. The assignment of weights for the *trans* BO_6 octahedron is straightforward; in the case of the *cis* octahedron we have chosen to weight both the bonds that form the chain and the bonds *trans* to them. The requirement for alternating bonds along the chain leads to a weighting that is counter to that suggested by the unweighted network equations. The predictions tend to underestimate the distortion in one direction and overestimate it in the other.

4. CONCLUSIONS

We have shown that d^0 transition metal cations in octahedral coordination are susceptible to out-of-center distortions in an amount that increases with increasing

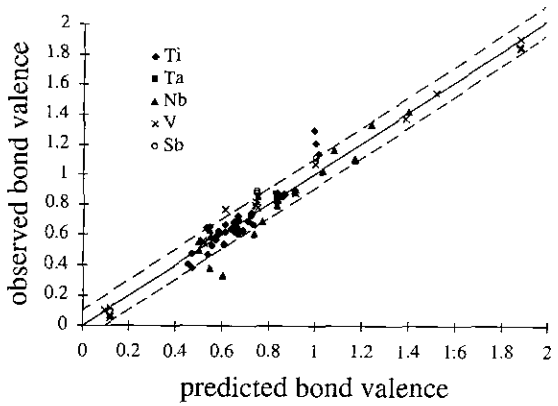

FIG. 6. Predicted bond valences versus observed bond valences for the bonds listed in Table 1. The lines show the region in which prediction and observation differ by less than 0.1 vu.

charge and decreases with increasing size. Whether a distortion will occur in a particular compound depends in part on the strength of the electronic effect (the HOMO–LUMO gap) and in part on the ability of the rest of the structure to support such a distortion. In most cases where an electronic distortion is found, the effect is also supported by a structural distortion caused by either the nature of the bond network, lattice stress, or cation–cation repulsion, and that the structural effects become larger as the electronic effect increases. Structural and electronic effects are mutually supportive and are not easy to separate.

The electronic effect itself does not determine in which direction the cation moves out of center. This is determined by the bond network or the cation–cation repulsion if these effects are present, otherwise the direction of displacement must break a symmetry of the structure and can occur in one of several possible directions. We have proposed a way of estimating the magnitude of the displacement using a form of weighted network equations with weights that are transferable between compounds of a given cation, and with these we have been able to reproduce reasonably well the observed distortions. Although we have examined a large number of different compounds, in this paper we have chosen to illustrate only a few simple related structures, to give a flavor for the kind of agreement that can be expected. This agreement is illustrated in Fig. 6, which plots the predicted against the observed bond valences from Table 1. In most cases, the predictions, which cover the range from 0.1 to 1.8 vu, lie within 0.1 vu of the observed values.

ACKNOWLEDGMENTS

M.K. thanks the "Schweizerische Nationalfonds" for a fellowship which allowed him to spend a year at McMaster University where this work was performed with the aid of a research operating grant awarded to I.D.B. by the Natural Science and Engineering Council of Canada.

REFERENCES

1. J. A. Speer and G. V. Gibbs, *Am. Mineral.* **61,** 238 (1976).
2. G. D. Stucky, M. L. F. Philips, and E. G. Thurman, *Chem. Mater.* **1,** 492 (1989).
3. P. A. Thomas, A. M. Glazer, and B. E. Watts, *Acta Crystallogr. Sect. B* **46,** 333 (1990).
4. R. E. Cohen, *Nature* **358,** 136 (1992).
5. I. D. Brown, *Acta Crystallogr. Sect. B* **44,** 545 (1988).
6. J. K. Burdett, "Molecular Shapes." Wiley–Interscience, New York, 1980.
7. R. A. Wheeler, M. H. Whangbo, T. Hughbanks, R. Hoffmann, J. K. Burdett, and T. A. Albright, *J. Am. Chem. Soc.* **108,** 2222 (1986).
8. M. Munowitz, R. H. Jarman, and J. F. Harrison, *Chem. Mater.* **5,** 661 (1993).
9. M. L. F. Philips, W. T. A. Harrison, T. E. Gier, G. D. Stucky, G. V. Kulkarni, and J. K. Burdett, *Inorg. Chem.* **29,** 2158 (1990).
10. S. K. Kang, H. Tang, and T. A. Albright, *J. Amer. Chem. Soc.* **115,** 1971 (1993).
11. G. Bergeroff, R. Hundt, R. Sievers, and I. D. Brown, *J. Chem. Inf. Comp. Sci.* **23,** 66 (1983).
12. I. D. Brown, *Acta Crystallogr. Sect. B* **48,** 553 (1992).
13. I. D. Brown and D. Altermatt, *Acta Crystallogr. Sect. B* **41,** 244 (1985).
14. I. D. Brown, *Z. Kristallogr.* **199,** 255 and Appendix (1992).
15. V. E. Zavodnik, E. A. Zhurova, and V. G. Tsirelson, *Z. Kristallogr,* in press.
16. Y. A. Abramov, V. E. Zavodnik, S. A. Ivanov, I. D. Brown, and V. G. Tsirelson, submitted for publication.